Journal of Geoscience and Environment Protection, 2024, 12, 110-130
https://www.scirp.org/journal/gep
ISSN Online: 2327-4344
ISSN Print: 2327-4336

Assessing the Relationship between October-November-December Rainfall and Indian Ocean Dipole in Recent Decades over Tanzania Following the 2011 Abrupt Change

Charles Yusuph Ntigwaza[1,2,3], Wen Wang[1]

[1]Key Laboratory of Meteorological Disaster of Ministry of Education (KLME)/International Joint Research Laboratory of Climate and Environment Change (ILCEC)/Collaborative Innovation Center on Forecast and Evaluation of Meteorological Disasters (CIC-FEMD), School of Atmospheric Sciences, Nanjing University of Information Science & Technology, Nanjing, China
[2]Tanzania Meteorological Authority, Dodoma, Tanzania
[3]National Meteorological Training Centre, Kigoma, Tanzania
Email: wangwen@nuist.edu.cn

How to cite this paper: Ntigwaza, C. Y., & Wang, W. (2024). Assessing the Relationship between October-November-December Rainfall and Indian Ocean Dipole in Recent Decades over Tanzania Following the 2011 Abrupt Change. *Journal of Geoscience and Environment Protection, 12,* 110-130.
https://doi.org/10.4236/gep.2024.123007

Received: February 2, 2024
Accepted: March 22, 2024
Published: March 25, 2024

Abstract

The present study explored how the Indian Ocean Dipole (IOD) influences October-November-December (OND) rainfall over Tanzania in recent decade following the 2011 abrupt change. The study spans 50 years, from 1973 to 2022. Notable abrupt changes were observed in 1976 and 2011, leading us to divide our study into two periods: 1976-2010 and 2011-2022, allowing for a close investigation into the existing relationship between OND IOD and OND rainfall and their associated large-scale atmospheric circulations. It was found that the relationship between OND IOD and OND rainfall strengthened, with the correlation changed from +0.73 during 1976-2010 to +0.81 during 2011-2022. Further investigation revealed that, during 1976-2010, areas that received above-normal rainfall during positive IOD experienced below-normal during 2011-2022 and vice versa. The same pattern relationship was observed for negative IOD. Spatial analysis demonstrates that the percentage departure of rainfall across the region mirrors the standardized rainfall anomalies. The study highlights that the changing relationship between OND IOD and OND rainfall corresponds to the east-west shift of Walker circulation, as well as the north-south shift of Hadley circulation. Analysis of sea surface temperature (SST) indicates that both positive and negative IOD events strengthened during 2011-2022 compared to 1976-2010. Close monitoring of this relationship across different timescales could be useful for updating OND rainfall seasonal forecasts in Tanzania, serving as a tool for reducing socio-economic impacts.

Keywords

Sea Surface Temperature (SST), Percentage Departure of Rainfall, Atmospheric Circulations, Walker Circulation, Hadley Circulation

1. Introduction

In recent decades, East Africa has witnessed a surge in extreme climate events, notably droughts and floods, with profound socio-economic ramifications (Anande & Luhunga, 2019; Kimambo et al., 2019; Lukali et al., 2021). Specifically, studies in Tanzania have highlighted an increased frequency of floods during the October-November-December (OND) rainy season (Mbigi & Xiao, 2021), in contrast to a decadal decrease in flood events during March-April-May (MAM) rainy season in the late 1990s (Makula & Zhou, 2022; Umutoni et al., 2021).

The variability in the OND rainy season in Tanzania is linked to diverse climate drivers, leading to substantial interannual variations compared to MAM rainy season (Ayugi et al., 2018; Black et al., 2003). Previous research attributes this variability to sea surface temperature (SST) in the tropical Indian Ocean, tropical Pacific Ocean, and tropical Atlantic Ocean (Wenhaji Ndomeni et al., 2018). Climate indices such as the Indian Ocean Dipole (IOD) and the El Niño Southern Oscillation (ENSO), among others, have been defined to understand these relationships (Ame et al., 2021; Kavishe & Limbu, 2020). Past investigations have explored the individual effects of IOD and ENSO (Clark et al., 2003; Saji & Yamagata, 2003) as well as their combined impacts (Ashok et al., 2004). During ENSO phases, El Niño (La Niña) events are associated with increased (reduced) OND rainfall, while positive (negative) IOD events are linked to above (below) normal OND rainfall (Wenhaji Ndomeni et al., 2018). Moreover, changes in the Walker circulation contribute to OND rainfall variability in Tanzania, directly linked to tropical SST and convection anomalies (Limbu & Guirong, 2020).

Studies classify climate drivers during the OND rainy season as interannual variability (e.g., IOD and ENSO) and interdecadal variability, connected to SST over the tropical central Indian Ocean and the Atlantic Ocean (Otte et al., 2017). In the Southern Hemisphere, atmospheric variations are predominantly mediated through the Southern Annular Mode (SAM) or Antarctic Oscillation (Prabhu et al., 2016; Thompson & Wallace, 2000). SAM influences OND rainfall by modulating the sea level pressure meridional dipole, impacting Mascarene high and leading to drought or weak flood events (Mbigi & Xiao, 2023; Peng et al., 2020; Xing & Ogou, 2015).

OND rainy season dynamics are influenced by diverse climate drivers, with impacts evolving over time. For instance, some studies report a positive response to El Niño, while others indicate a negative response (Ayugi et al., 2018; Mafuru

& Guirong, 2020). According to Kebacho (2021), the highest number of heavy rainfall events (HREs) during OND rainy season in 2011 was observed over the Lake Victoria basin and northern coast zones while the north eastern highlands received the least amount. The influence of IOD on the OND rainy season in Tanzania has been a subject of investigation, with varying findings highlighting the complexity of IOD's impact on regional climate dynamics. Notably, there is a paucity of documentation on the recent status of OND rainfall in relation to Indian Ocean in Tanzania, particularly regarding the abrupt rainfall trend change in 2011. This abrupt change in 2011 marked a significant shift in OND rainfall patterns, impacting communities, agriculture, and ecosystems across Tanzania. This prompts questions about the pre- and post-2011 periods, the consistency of the relationship between OND rainfall and IOD, and the conditions for wet and dry events during IOD phases before and after 2011. Given the significance of accurately predicting rainfall in the region, there is a compelling need to investigate the interaction between OND rainy season and influencing climate drivers over different decades. This study aims to assess the relationship between OND rainy season and OND IOD over Tanzania in recent decade following the 2011 abrupt change, focusing on two periods: 1976-2010 and 2011-2022. The investigation seeks to understand how the relationship between OND rainfall and OND IOD evolved after the abrupt change in 2011, addressing the spatial and temporal variability, the connection between IOD and rainfall, and the underlying physical mechanisms affecting OND rainfall in Tanzania. The outcomes of this study are crucial for enhancing the understanding of rainfall variability and its drivers, ultimately improving the prediction of OND rainfall events in Tanzania. This knowledge can aid stakeholders and the community in implementing effective mitigation measures to alleviate the adverse impacts of climate-related disasters, including flooding and drought. The subsequent sections of this study will detail the study area, data, and methods (Section 2), present results and discussions (Section 3), and conclusion (Section 4).

2. Study Area, Data and Methods

2.1. Study Area

Tanzania is an equatorial tropical country located in eastern Africa, bounded between 28˚E-42˚E longitude and 12˚S-0˚ latitude. The country features complex topographic variations, ranging from low coast plain areas in the east to highlands in the southern and northeastern parts. To the east, Tanzania is bounded by the Indian Ocean, the primary source of moisture. It is also surrounded by Mount Kilimanjaro in the northeastern part, which is the highest mountain in Africa with an altitude of 5895 m, Lake Victoria to the north, Lake Tanganyika to the west and Lake Nyasa to the south (**Figure 1**).

Climatologically, rainfall distribution across Tanzania during the OND rainy season varies from place to place. The western part and the Lake Victoria basin experience more significant rainfall (more than 75 mm per month), followed by

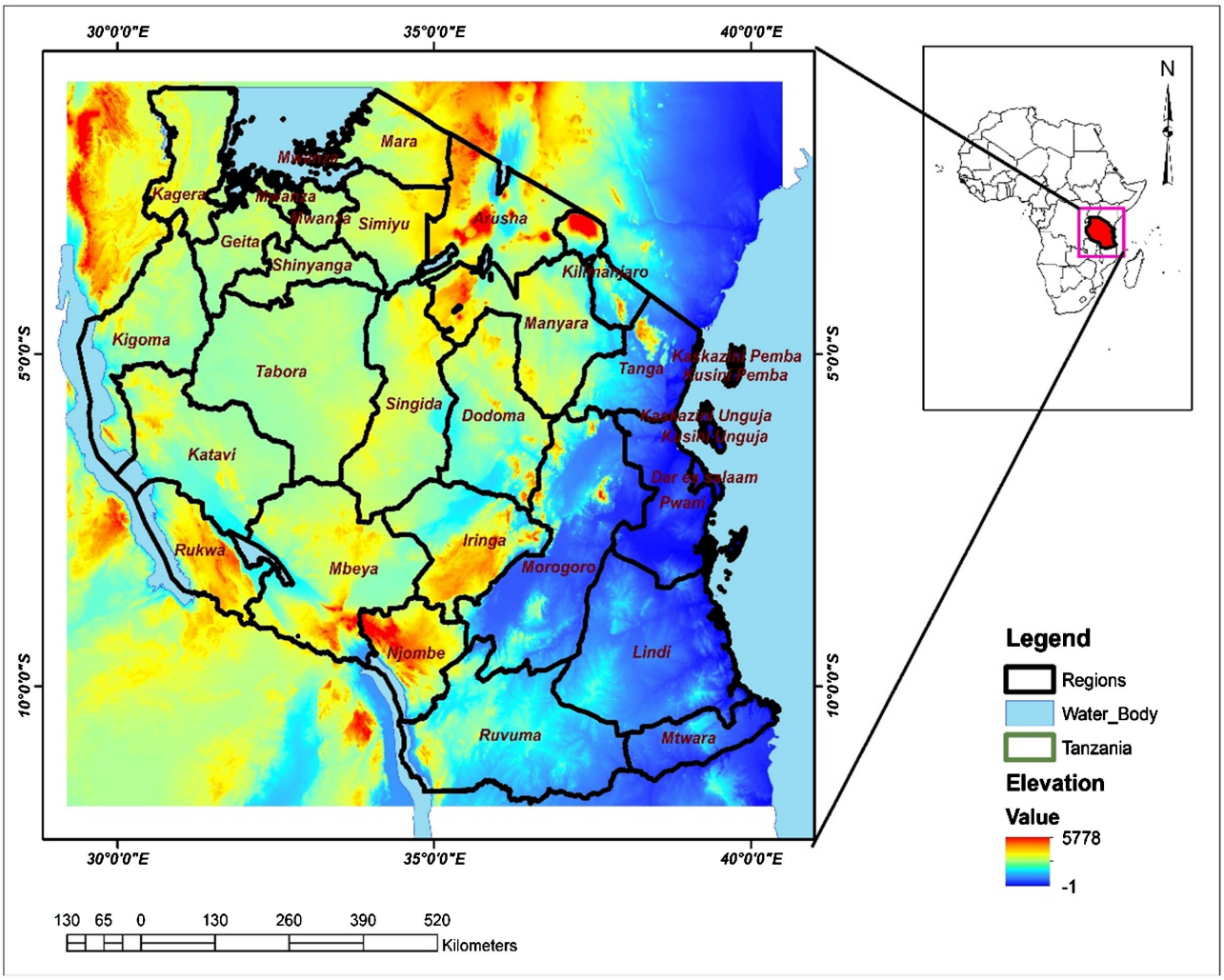

Figure 1. Topographical map of Tanzania showing elevation distribution over the country.

the southern and eastern regions. In contrast, the central areas, northeastern and southwestern highlands receive lesser amount of rainfall (less than 75 mm per month) (**Figure 2**). The presence of the Congo airmass, Lake Tanganyika, and Lake Victoria creates a conducive environment for rainfall formation, influencing the early onset of OND rainfall over the western and northern Tanzania by supplying ample moisture (Makula & Zhou, 2022).

2.2. Data

The present study employs a combination of different monthly mean meteorological variable reanalysis datasets. These include precipitation from the Climatic Research Unit (CRU) of the University of East Anglia (Harris et al., 2020). It is the latest version 4.07 dataset (CRU TS 4.07) with a horizontal resolution of 0.5˚ × 0.5˚ latitude-longitude grid and covers a longer period of time. Its performance over the study domain has been assessed (Koutsouris et al., 2016). Other scholars have applied it to examine rainfall variability over the study domain, making it suitable for this study (Borhara et al., 2020; Makula & Zhou, 2022;

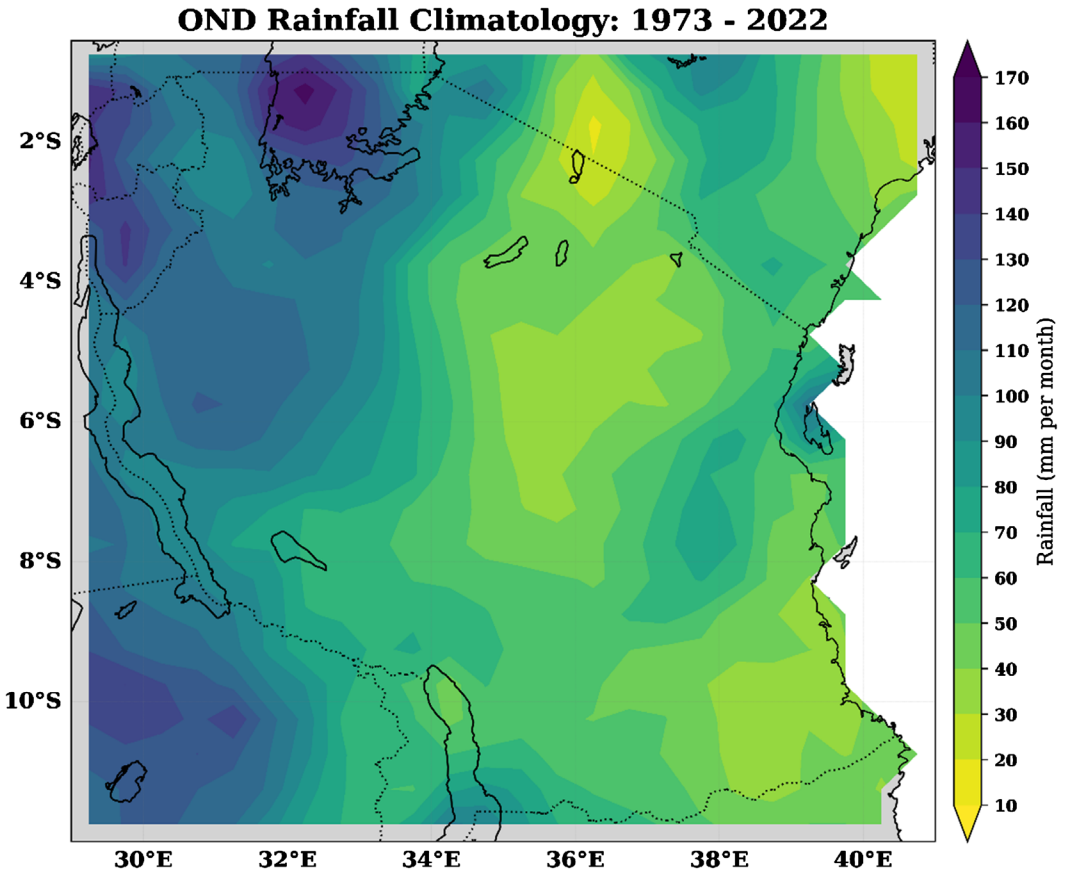

Figure 2. Map of seasonal climatological distribution of OND rainfall distribution (mm per month) in Tanzania during 1973-2022.

(Mbigi & Xiao, 2021).

The study also used version 5 of Extended Reconstructed SST (ERSSTv5) offered by the National Oceanic and Atmospheric Administration (NOAA) (Huang et al., 2017). ERSSTv5 has a spatial resolution of 2.0˚ by 2.0˚ and has been applied by other scholars to study the same over the study domain (Makula & Zhou, 2022). Moreover, study utilized atmospheric datasets, namely zonal wind, meridional wind, velocity potential and vertical velocity (omega), form the National Centres for Environment Prediction-National Centre for Atmospheric Research (NCEP-NCAR) reanalysis (Kalnay et al., 1996; Kistler et al., 2001). These are reanalysis datasets with a spatial resolution of 2.5˚ × 2.5˚ and have been used in different studies to explain the atmospheric circulation over the study domain (Makula & Zhou, 2022; Umutoni et al., 2021; Vigaud et al., 2018).

2.3. Methods

The study employed a number of methods scientifically approved by different studies to perform better over the region. Sequential Mann-Kendall method, a nonparametric test, was applied to detect the change of point of a long-term time series of precipitation data (Sneyers, 1990). It incorporates the sequential progressive and retrograde standardized curves denoted by $U(t)$ and $U'(t)$

respectively. $U(t)$ and $U'(t)$ are both calculated by Equation (1); their only difference is that $U'(t)$ is calculated starting from the end of the sequence.

$$U(t) = \frac{t_i - E(t)}{\sqrt{Var(t_i)}} \tag{1}$$

where $E(t)$ and $Var(t)$ are the mean and variance, respectively, obtained at every statistic test t from $i = 1$ up to the total number of events in the sequence (N).

When the two curves are plotted, their point of intersection provides an approximate potential trend change within the time series. When the point of intersection occurs beyond ±1.96 of the standardized statistic (t) at a 95% confidence level, a detectable change at that point in the time series can be established. At such a point, the change is said to be significant, marking the start year of the trend (Mosmann et al., 2004).

On the other hand, IOD index was defined basing on SST anomalies over the Indian Ocean as the difference between the SST anomalies of the western (50˚E-70˚E, 10˚S-70˚N) and eastern (90˚E-110˚E, 0˚-10˚S) tropical Indian Ocean (Saji et al., 1999). To account for the impact of climate change, the influence of basin warming was removed by detrending the SST anomaly. The years were defined as positive (negative) IOD when the detrended OND SST anomalies were greater (smaller) than 0.5 (−0.5)˚C, otherwise it was regarded as a neutral year (Ashok et al., 2004; Kebacho, 2021; Yamagata et al., 2013).

In order to understand how the relationship between OND rainy season and OND IOD is varying recently as compared to some decades ago, two periods were chosen based on Mann-Kendall Sequential trend test results. For the two chosen periods, all the anomalies were generated with respect to 1991-2020 climatology according to World Meteorological Organization (WMO) definition. To understand the impact of IOD over the study domain, the composite analysis for positive and negative IOD events were generated for the two selected periods. Percentage departure precipitation as calculated by Equation (2), was applied to confirm the validity of rainfall anomalies and to check how the rainfall distribution has changed during the two categorized periods. The composite anomalies of OND rainfall, SST, velocity potential along with divergent wind, Walker and Hadley circulations were investigated. The statistical significance of the composite analysis was identified based on Student's t-test (Equation (3)).

$$P_d = \frac{x_i - \overline{x}}{\overline{x}} * 100\% \tag{2}$$

$$t = \frac{r_{xy} \times \sqrt{N-2}}{\sqrt{1-r_{xy}}} \tag{3}$$

where r_{xy} stands for correlation between two variables x and y, N is the total number of observed events, t is the test statistic, $\overline{x}$ is the mean value of x and P_d is the percentage departure of precipitation.

3. Results and Discussion

3.1. Determining the OND Rainfall Trend Change Point

During the study period, Sequential Mann-Kendall trend test results for OND rainfall shows two significant abrupt shifts in 1976 and 2011 (Figure 3). As shown in Table 1, both 1976 and 2011 are neutral years. Past studies have associated the abrupt change in 1976 with a shift to a warmer state in the tropical oceans (Trenberth & Hoar, 1996), leading to interdecadal variability in East Africa OND rainfall (Clark et al., 2003). It was further reported that the heavy rainfall over northern Tanzania in 2011 was associated with moisture flux convergence (Kebacho, 2021). This implies that the two identical abrupt changes during the study period might be associated with different atmospheric circulations.

Based on the findings of this study, two periods were chosen to understand how the relationship between OND rainfall and OND IOD is currently varying compared to some decades ago. These are of 35 years from 1976 to 2010 and 12 years starting from 2011 to 2022.

3.2. Classification of IOD, Wet and Dry Events

Through calculations and as depicted in Figure 4 and Table 1, it was found that the two periods exhibited a different number of positive and negative IOD events. The correlation between OND IOD and OND rainfall was found to be +0.73 (+0.81) during 1976-2010 (2011-2022). The study identified 6 positive IOD events during 1976-2010 compared to 3 events during 2011-2012. This means that, during 1976-2010, positive IOD events accounts for 66.7% while during 2011-2022 accounted to 33.4%. Thus, the positive IOD events decreased

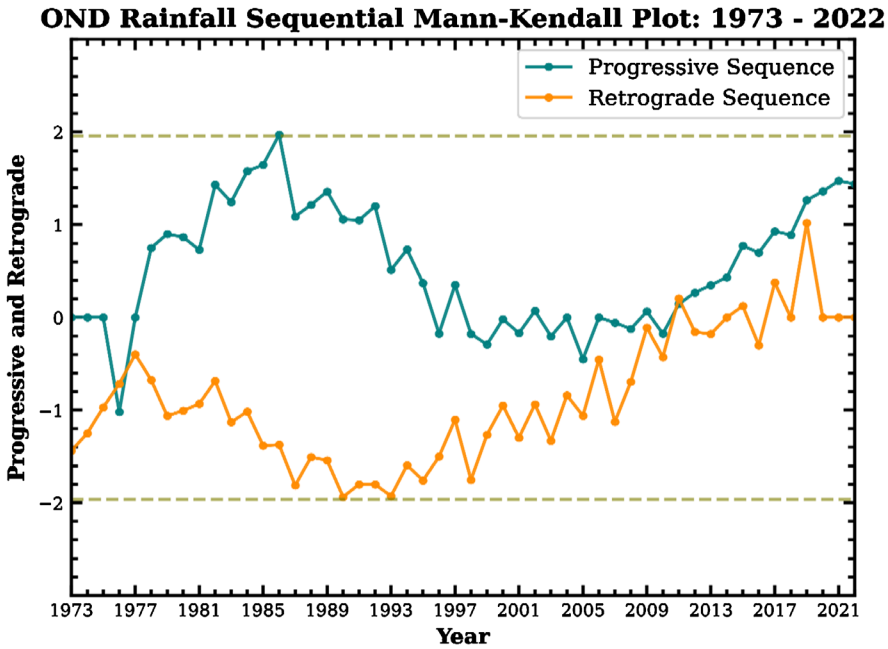

Figure 3. Sequential Mann-Kendall trend test of OND rainfall over Tanzania during 1973-2022.

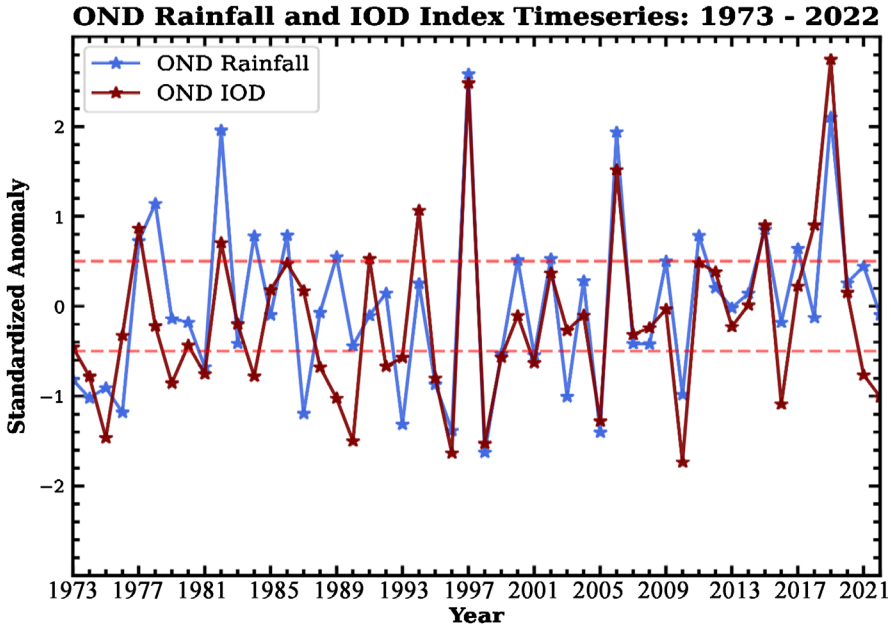

Figure 4. Normalized time series of OND rainfall over Tanzania (blue) and IOD index (red) during 1973-2022. The dashed line indicate the threshold values of +0.5 and −0.5 for positive and negative IOD, respectively.

Table 1. Classification of IOD events during Period 1: 1976-2010 and Period 2: 2011-2022.

Positive IOD	Period 1	1977, 1982, 1991, 1994, 1997, 2006
	Period 2	2015, 2018, 2019
Negative IOD	Period 1	1979, 1981, 1984, 1988, 1989, 1990, 1992, 1993, 1995, 1996, 1998, 1999, 2001, 2005, 2010
	Period 2	2016, 2021, 2022

by 33.4% during 2011-2022 compared to 1976-2010. On the other hand, there were 9 negative IOD events during 1976-2010 equal to 83.3%, compared to 3 events during 2011-2022, equal to 16.7%. This also implies that negative IOD events decreased by 66.6% during 2011-2022 as compared to 1976-2010.

The findings of the study align with two famous OND rainfall extreme events which were previously reported: the 1997 extreme event that was due to the combined effect of positive IOD and warm phase of ENSO and the 2019 extreme event that was attributed to the positive phase of IOD (Chang'a, Kijazi, Mafuru, Kondowe et al., 2020). The study found that the correlation between OND rainfall and IOD was +0.73 (+0.81) during 1976-2010 (2011-2022). This indicates that the relationship between them strengthened during 2011-2022 compared to 1976-2010. Furthermore, the study found that during 2011-2022 there was only one wet event (2019) compared to five (5) wet events (1978, 1982, 1986, 1997 and 2006) during 1976-2010. The study found no dry event during 2011-2022, with eight (8) dry events (1976, 1987, 1993, 1996, 1998, 2003, 2005 and 2010) during 1976-2010 (**Figure 4**). The selection of wet (dry) years was based on the threshold value of standardized rainfall anomalies of $>1(<-1)\sigma$. The same de-

finition has been used by other scholars to perform the same over the study domain (Mbigi & Xiao, 2021). The findings conform to what was reported by past researchers (Limbu & Tan, 2019). Further analysis regarding to the abrupt change and how IOD influences rainfall are discussed in the next section.

3.3. Relationship between IOD and OND Rainy Season

3.3.1. Composites of Rainfall Anomaly

The composites of OND standardized rainfall anomalies corresponding to positive IOD and negative IOD for the two chosen periods are depicted in **Figure 5**. The positive IOD composites during 1976-2010 (**Figure 5(a)**) show above-normal all over the region, with largest significant values in the eastern part. Meanwhile, the northern part of the country around Lake Victoria basin was observed to have above normal nonsignificant amounts. The results were opposite during 2011-2022, whereby the northern part was observed to have largest above-normal significant

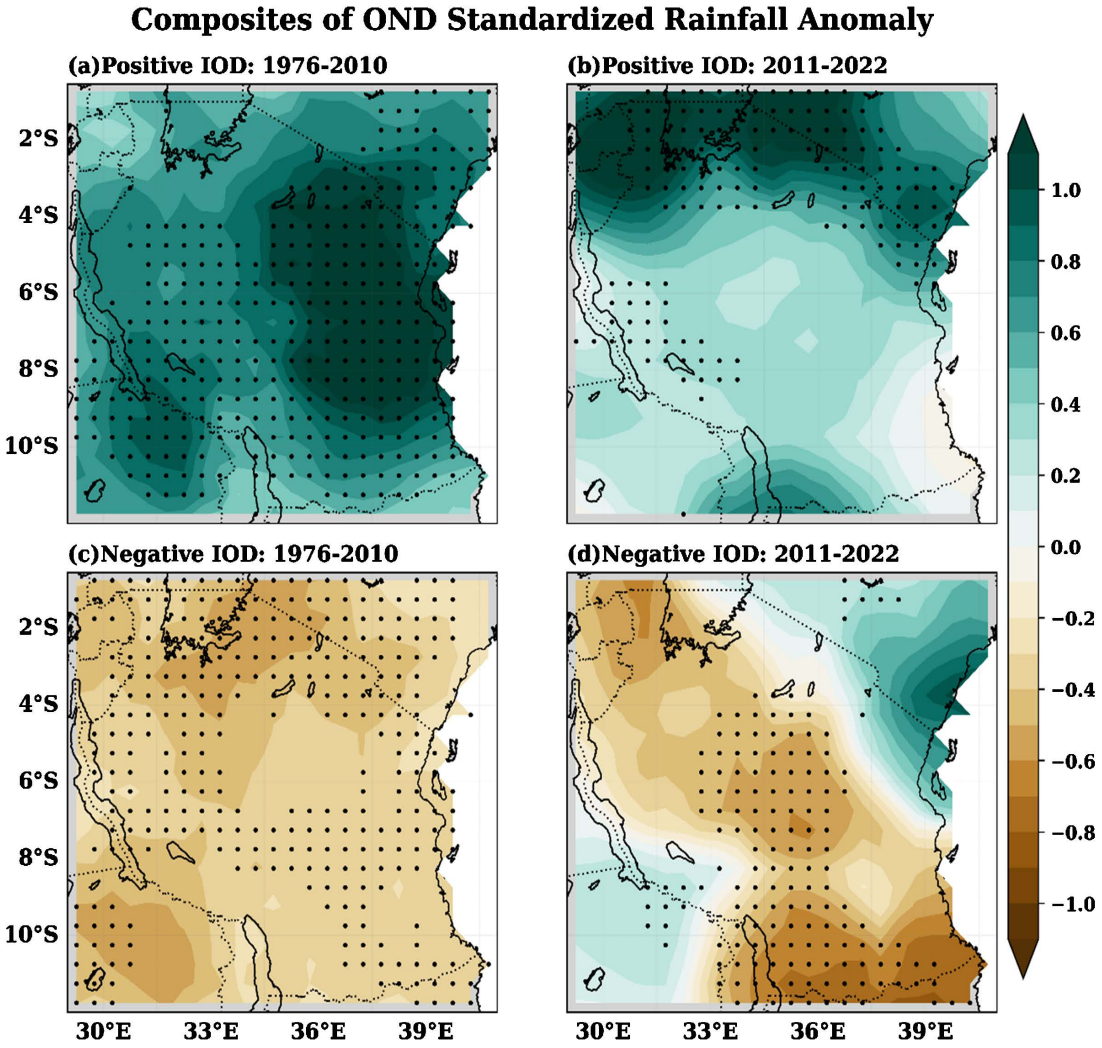

Figure 5. Composites of OND rainfall standardized anomaly for (a) 1976-2010 (b) 2011-2022 during positive IOD. (c) and (d) are the same as (a) and (b) but during negative IOD. Dotted areas represent significant standardized anomaly values at 95% confidence level based on Student's t test.

values compared to the eastern part, which shows below-normal nonsignificant values (Figure 5(b)).

On the other hand, negative IOD composites during 1976-2010 show below-normal significant values in most parts of the country, with the largest values being on the northern part, while the central and southwestern parts show nonsignificant values (Figure 5(c)). During 2011-2022, northeastern and southwestern parts show above-normal values, while the rest of the country shows below-normal values, with significant values over the central and southern (largest values) parts (Figure 5(d)).

The most important point to note here is that for positive IOD events, some areas such as the northern (western) part, which received less(much) amount of rainfall during 1976-2010, received much(less) rainfall during 2011-2022 (Figure 5(a) & Figure 5(b)). For negative IOD events, the northeastern and southwestern parts turned from below average during 1976-2010 (Figure 5(c)) to above average during 2011-2022 (Figure 5(d)). This implies that there is a changing relationship between OND IOD and OND rainfall across different places over the study domain.

3.3.2. Composites of Rainfall Departure Percentage

In order to confirm the validity of rainfall distribution over the study domain, as shown on Figure 5, we determined percentage departure for composites of OND rainfall during the two periods (Figure 6). The two figures (Figure 5 & Figure 6) show the same rainfall patterns. Positive IOD composites during 1976-2010 show above-normal all over the region, with largest significant values in the eastern part. The northern part of the country around Lake Victoria basin was observed to have above normal nonsignificant percentage departure values. The results were a bit different during 2011-2022, whereby the northern part was observed to have above-normal significant percentage departure values compared to the eastern part, which shows below-normal percentage departure nonsignificant values (Figure 6(b)).

Furthermore, negative IOD composites during 1976-2010 show below-normal significant percentage departure values in most parts of the country (Figure 6(c)). During 2011-2022, northeastern and southwestern parts show above-normal percentage departure values, while the rest of the country shows nonsignificant below-normal values, with an exception of the central part which show significant values (Figure 6(d)).

More interesting, for positive IOD composites, some of the areas such as the northern part, which had nonsignificant positive percentage departure rainfall during 1976-2010 (Figure 6(a)), observed to have significant positive percentage departure values during 2011-2022 (Figure 6(b)). For negative IOD events, the northeastern and southwestern parts which was observed to be below-normal percentage departure during 1976-2010 (Figure 6(c)) turned to above-normal percentage departure during 2011-2022 (Figure 6(d)), the same as features observed in rainfall anomalies (Figure 5(a) & Figure 5(b)).

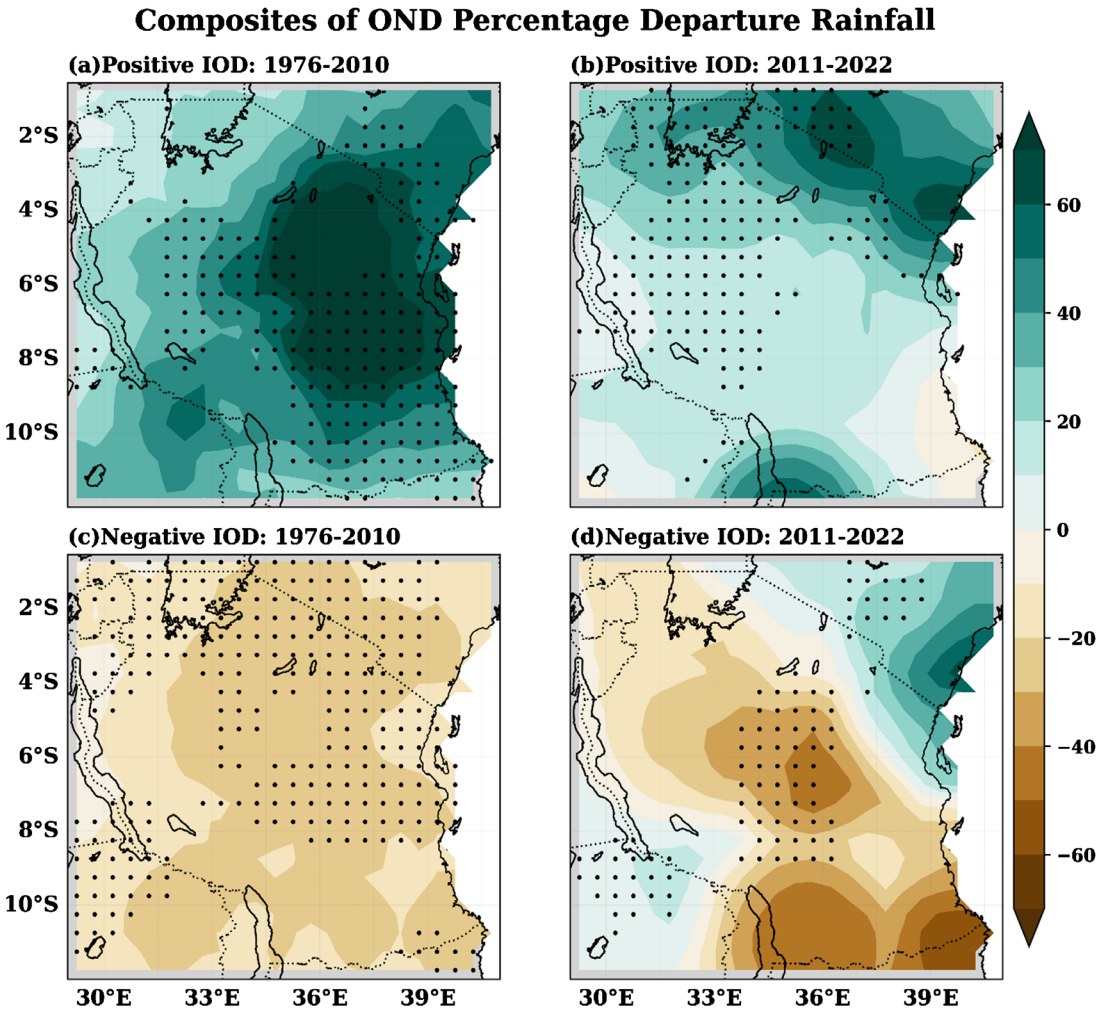

Figure 6. Composites of rainfall percentage departure over Tanzania for (a) 1976-2010 (b) 2011-2022 during positive IOD. (c) and (d) are the same as (a) and (b) but during negative IOD. Dotted areas represent significant percentage departure values at 95% confidence level based on Student's t-test.

3.4. Mechanisms behind the Changing Relationship between IOD and OND Rainfall

The study also investigated the differences between positive IOD and negative IOD composites by examining the corresponding SST anomalies, velocity potential along with divergent wind anomalies as well as Walker and Hadley circulations. The investigated mechanisms could build the basis for understanding the factors that contributes to the changing relationship between OND IOD and OND rainfall over the study area.

3.4.1. Sea Surface Temperature

Figure 7 displays the composite of detrended OND sea surface temperature anomalies (SSTA) corresponding to positive IOD and negative IOD years for the two chosen periods. During positive IOD, the SSTA composite shows a wider warm pool over the western Indian Ocean during 2011-2022 (Figure 7(b)) compared to that of 1976-2010 which was cooler on the southwestern part (Figure 7(a)). For

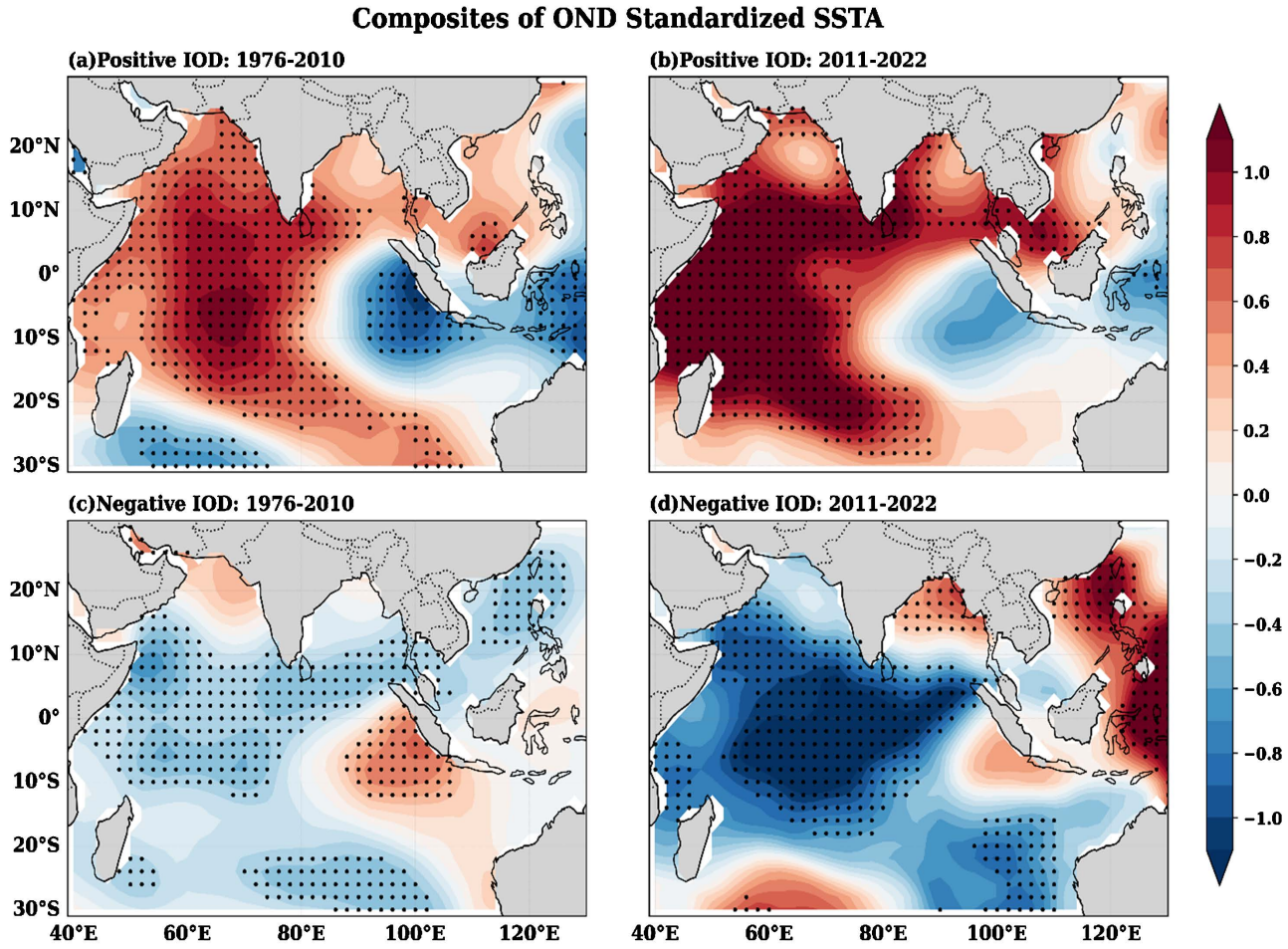

Figure 7. Composites of OND detrended standardized SSTA for (a) 1976-2010 (b) 2011-2022 during positive IOD. (c) and (d) are the same as (a) and (b) but during negative IOD. Anomalies were calculated basing on 1991-2020 climatology. Dotted areas represent significant standardized anomaly values at 95% level of confidence based on Student's t-test.

negative IOD composites, the central Indian Ocean was observed to be cooler during 2011-2022 (Figure 7(d)) compared to 1976-2010 (Figure 7(c)). Shifting of warmer cooler patterns was also noticed, for example, the northwestern part which was warmer during 1976-2010 (Figure 7(c)) was observed to be cooler during 2011-2022 (Figure 7(d)). The same phenomenon was observed over the northeastern part. Furthermore, the southwestern part of Indian Ocean which was cooler during 1976-2010 turned to warmer during 2011-2022 (Figure 7(c) & Figure 7(d)). Due to temperature differences, positive IOD is accompanied by easterly winds while negative IOD is accompanied by westerly wind at the surface.

The findings shows that both negative and positive IOD events strengthened, with the cautionary note that some areas turned from cooler to warmer while others from warmer to cooler during the two periods.

3.4.2. Velocity Potential and Divergent Wind

1) Velocity Potential and Divergent Wind at 850 hPa

In order to understand the influencing factor mechanisms behind the observed rainfall patterns, positive and negative IOD composite anomalies of ve-

locity potential along with divergent wind vectors at the 850 hPa pressure level were analyzed during the two periods (Figure 8). During 1976-2010, positive IOD composite anomalies show convergence over the central Pacific, America and western part of Indian Ocean including Tanzania while divergence was observed to cover the western Pacific (Southern Asia and Australia) and western Africa (Figure 8(a)). Both convergence and divergence were found to be shifting eastward, indicating the eastward shift of the Walker circulation but with a weaker strength during 2011-2022, with an exception over the Atlantic Ocean, where divergence was enhanced (Figure 8(b)).

Moreover, negative IOD events shows divergence over central and eastern Pacific as well as western Indian Ocean including Africa and Tanzania, while convergence was observed over the western Pacific (Figure 8(c)). Contrary to what was observed during positive IOD events, during 2011-2022, both convergence and divergence were enhanced and noticed to shift westwards, indicating the westward shift of the Walker circulation (Figure 8(d)). A northward shift of systems was also evident, indicating the northward shift of the Hadley circulation (Figure 8).

2) Velocity Potential and Divergent Wind at 200 hPa

In order to understand the mechanisms behind the observed rainfall patterns,

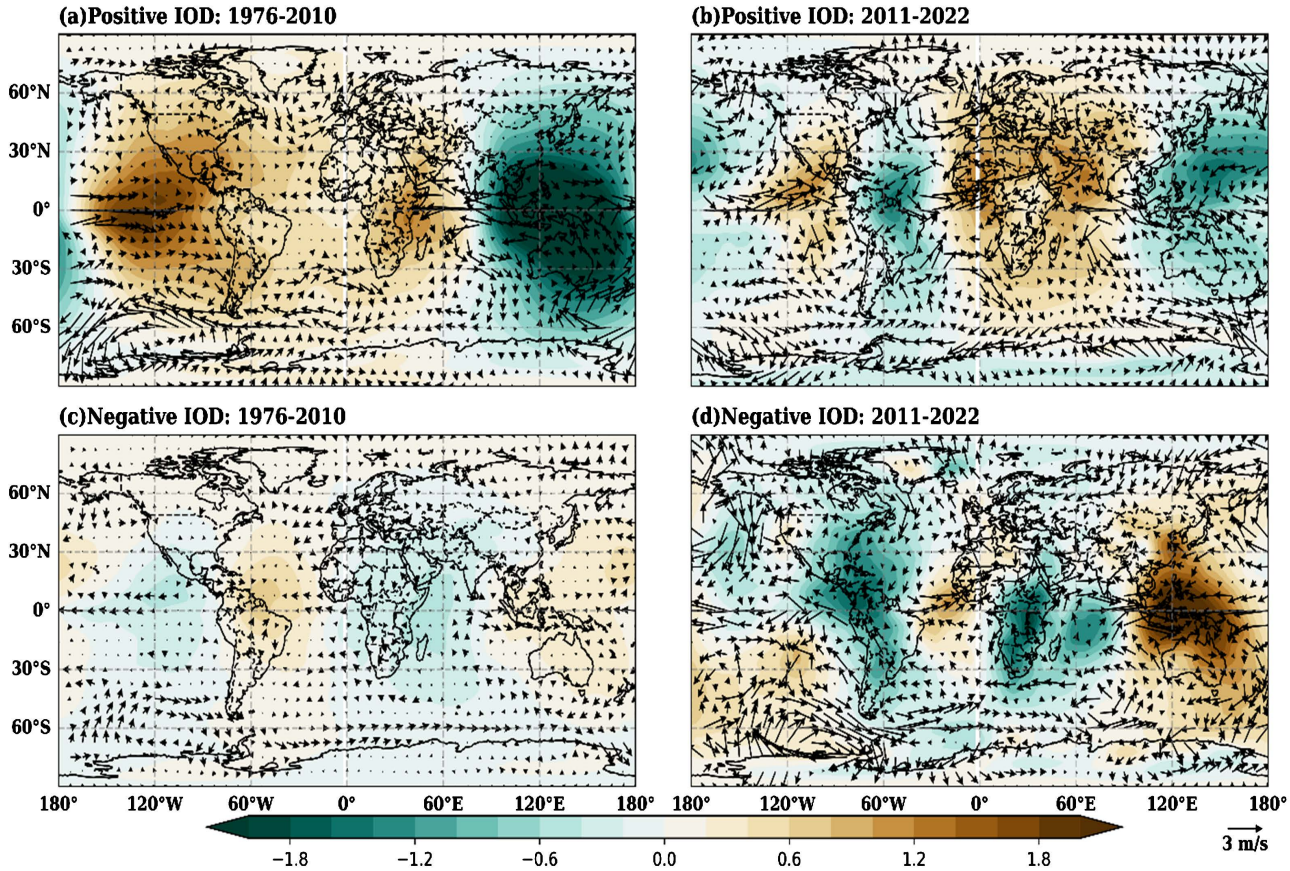

Figure 8. Velocity Potential anomaly composites (shading: 10^6 $m^2 \cdot s^{-1}$) along with divergent wind (ms^{-1}) plotted at 850 hPa for (a) 1976-2010 (b) 2011-2022 during positive IOD. (c) and (d) are the same as (a) and (b) but during negative IOD.

positive and negative IOD composite anomalies of velocity potential along with divergent wind vectors at the 200 hPa pressure level were also analyzed during the two periods (Figure 9).

During 1976-2010, positive IOD composite anomalies shows divergence over the central Pacific, America, as well as over western Indian Ocean, including Tanzania while convergence was observed to cover the western Pacific (including Southern Asia and Australia) and western Africa (Figure 9(a)). Both convergence and divergence were found to be shifting westwards, indicating the westward shift of the Walker circulation but with a weaker strength during 2011-2022, with an exception over the Indian Ocean and Atlantic Ocean, where the convergence were enhanced (Figure 9(b)). The convergence and divergence systems also exhibited a bit northward shift, especially over Indian Ocean, indicating a northward propagation of the Hadley circulation (Figure 9(b)).

On the other hand, during 1976-2010, negative IOD events shows convergence over central Pacific and western Indian Ocean, including Africa and Tanzania, while divergence was observed over the western Pacific (including Southern Asia and Australia) (Figure 9(c)). Contrary to what was experienced during positive IOD events, during 2011-2022, both convergence and divergence were enhanced and noticed to shift eastward, indicating the eastward shift of the Walker circulation (Figure 9(d)). A southward shift of systems was also noticeable,

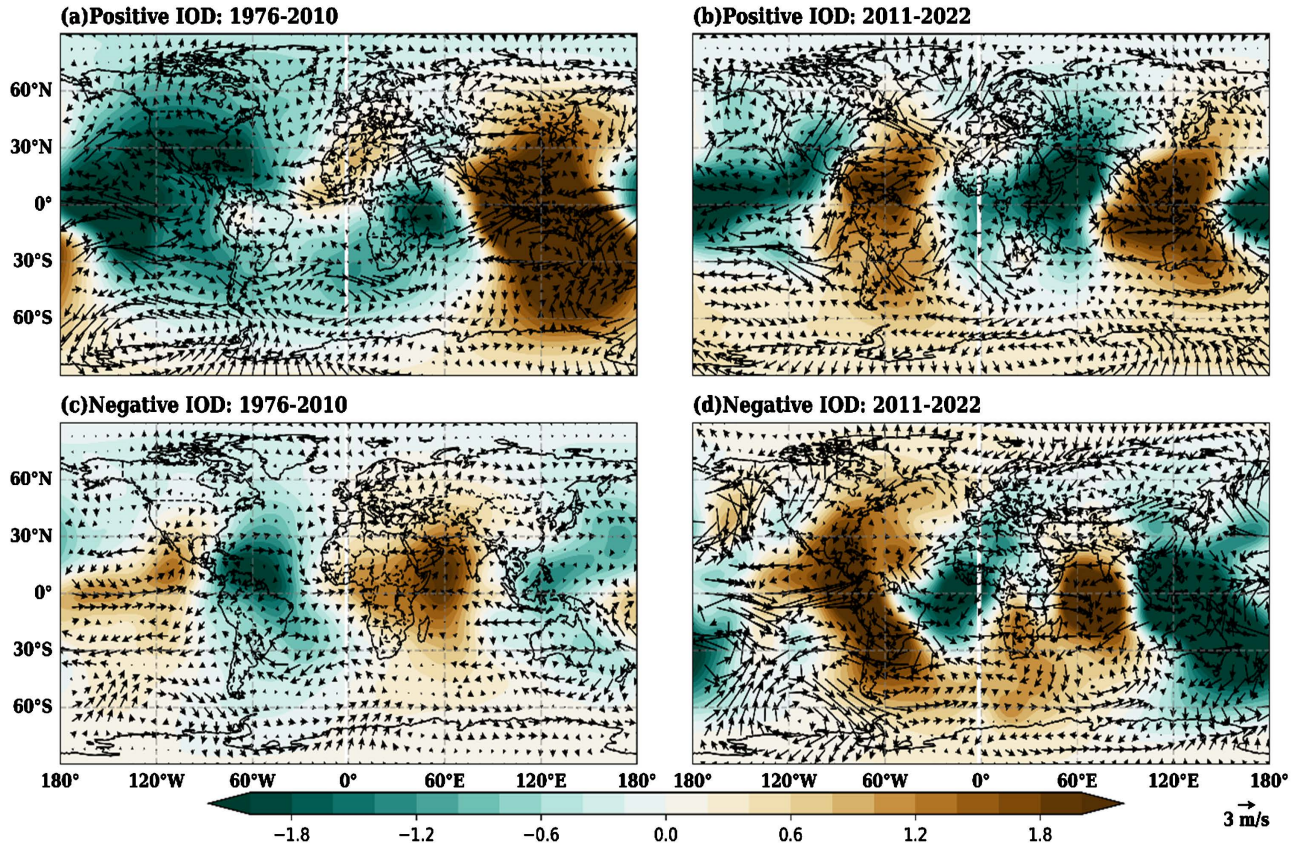

Figure 9. Velocity potential anomaly composites (shading: 10^6 $m^2 \cdot s^{-1}$) along with divergent wind (ms^{-1}) plotted at 200 hPa for (a) 1976-2010 (b) 2011-2022 during positive IOD. (c) and (d) are the same as (a) and (b) but during negative IOD.

indicating the southward shift of the Hadley circulation (**Figure 9**).

Generally, the study proposes that the changing relationship between IOD and OND rainfall might be attributed by the east-west (north-south) shifting of Walker (Hadley) circulation, which, on the other hand, due to teleconnection, changed the upper-level velocity potential and divergent wind systems, thus impacting the rainfall distribution over the region (**Figure 5**). The study observed that the lower and upper-level velocity potential & divergent wind systems were weakened (enhanced) during positive (negative) IOD on 2011-2022 as compared to 1976-2010 (**Figure 8** & **Figure 9**). The same atmospheric circulations were evident on **Figure 8** whereby the IOD structure favors westerly winds during positive IOD while negative IOD is accompanied by easterly winds. Past researchers have associated the position of Walker circulation with HREs over the northern part of Tanzania, in such a way that when its ascending limb is around 60˚E, it suppresses HREs (Japheth et al., 2021).

3.4.3. Walker Circulation

Additionally, the study analyzed the Walker and Hadley circulations. To account for the contribution of the Pacific Ocean wind patterns to the OND rainfall variability over Tanzania, we compare the east-west Walker circulation patterns over the Indo-Pacific region (**Figure 10**).

During positive IOD composites, the western Pacific was generally dominated by a strong (weak) ascending limb during 1976-2010 (2011-2022) (**Figure 10(a)** & **Figure 10(b)**), which appears to enhance the amount of rainfall over Tanzania (**Figure 5(a)** & **Figure 5(b)**). However, during 1976-2010, Tanzania was characterized by descending limb (**Figure 10(a)**) compared to 2011-2022, whereby ascending motion dominated the area (**Figure 10(b)**). Contrary to what was observed during positive IOD events, the western Pacific was dominated by a descending limb during negative IOD events (**Figure 10(c)** & **Figure 10(d)**). During the time, Tanzania was ruled by a descending (ascending) limb during 1976-2010 (2011-2022) (**Figure 10(c)** & **Figure 10(d)**), suppressing (enhancing) the amount of rainfall specifically in the southwestern and northeastern parts of our study domain (**Figure 5(c)** & **Figure 5(d)**).

It has been documented that the ascending limb of the Walker circulation over the study domain enhances convection, with the strongest uplift accompanied by convective activity of the moisture flux from the Congo airmass and that from the tropical Indian Ocean leading to anomalous rainfall over Tanzania (Limbu & Tan, 2019).

3.4.4. Hadley Circulation

As depicted in **Figure 11(a)** & **Figure 11(b)**, the study found that during positive IOD events, the Hadley circulation generally show a strong (weak) ascending motion over the study domain during 1976-2010 (2011-2022). This was also evident in the velocity potential and divergent wind, which explained about Hadley circulation shift towards the north and its role as a moisture supplier

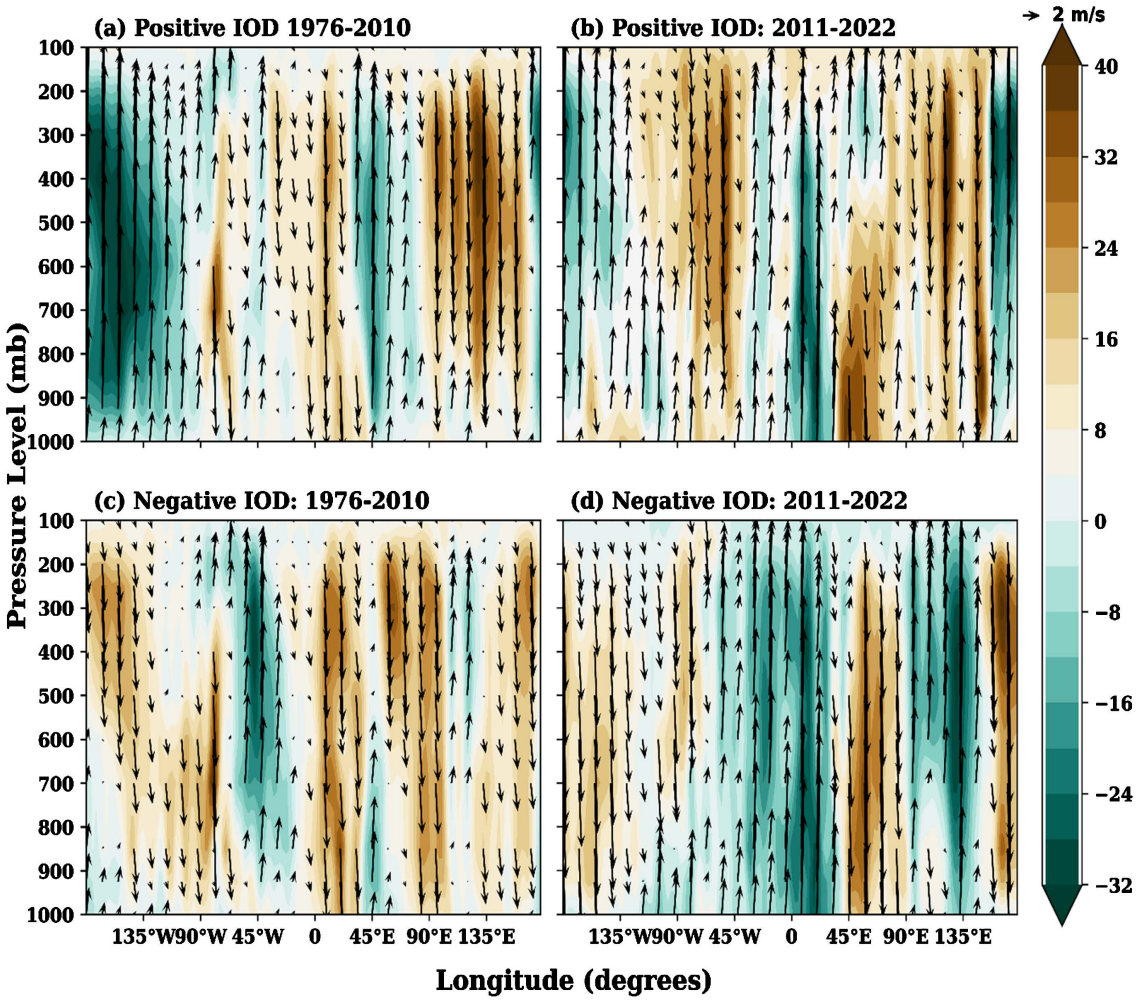

Figure 10. Walker circulation anomalies for (a) 1976-2010 (b) 2011-2022 during positive IOD. (c) and (d) are the same as (a) and (b) but during negative IOD. Vector plotted using zonal wind (u) and vertical velocity (omega) from 1000 hPa to 100 hPa. Values were averaged over latitude 5˚S-5˚N to suit Tanzania. Color contouring represents omega 10^3 ms^{-1}.

over the study domain (Figure 9(a) & Figure 9(b)). This impact resulted in an enhanced amount of rainfall during 1976-2010 compared to 2011-2022 (Figure 5(a) & Figure 5(b)).

During negative IOD events, the Hadley circulation showed that the study domain was generally dominated by descending motion during 1976-2010 (Figure 11(c)), while the findings were opposite during 2011-2022, whereby ascending motion was evident (Figure 11(d)). This caused the study domain to experience anomalous rainfall, especially in the southwestern and northeastern parts, where above-normal rainfall was observed, leaving the rest of the country below normal (Figure 5(d)).

Past studies have documented that Hadley circulation over the Indian landmass is recognized as a meridional overturning circulation in which hot air rises at the equatorial region and moves poleward, where it cools, sinks and moves back to the equator (Sharma et al., 2023). This coupled air-sea feedback over

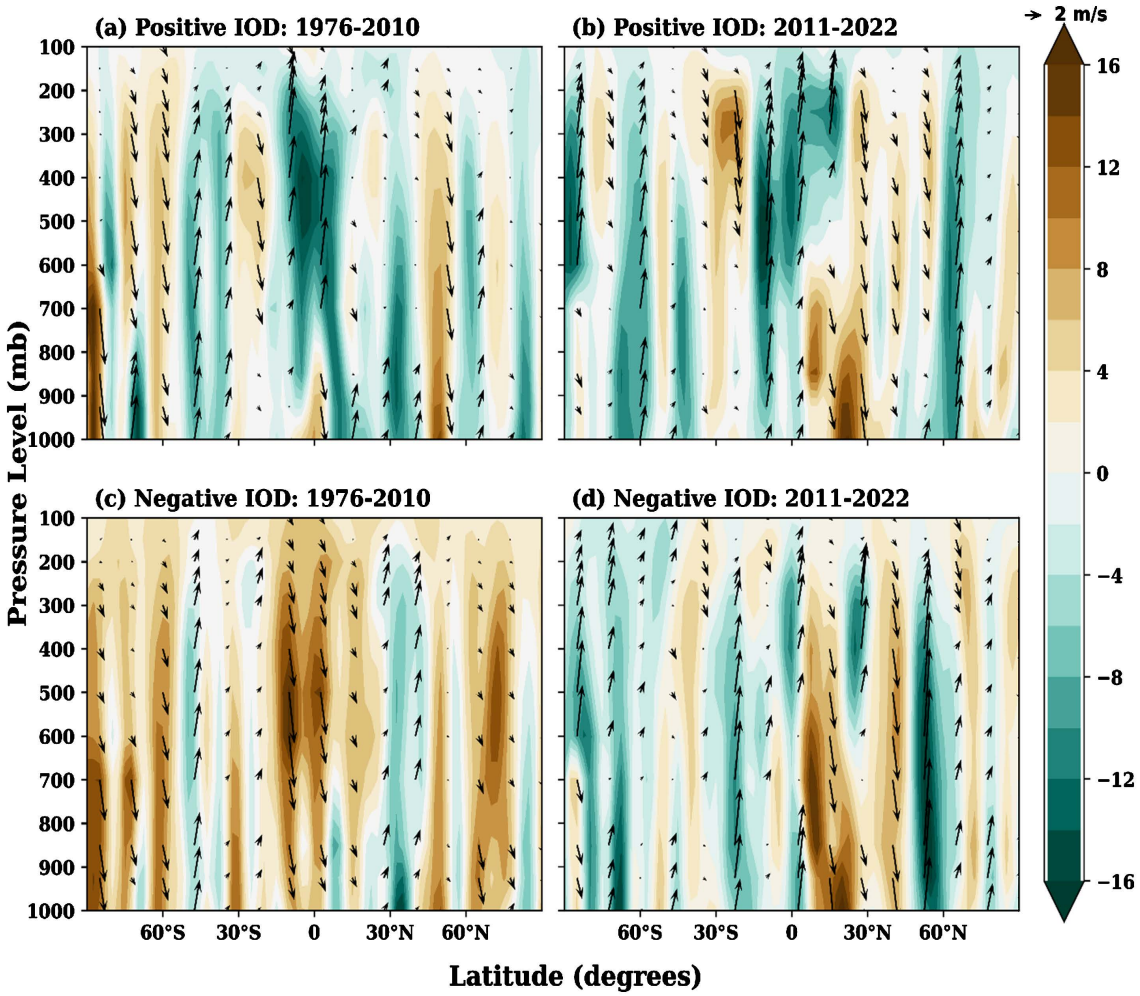

Figure 11. Hadley circulation anomalies over part of Indian Ocean and landmass for (a) 1976-2010 (b) 2011 during positive IOD. (c) and (d) are the same as (a) and (b) but during negative IOD. Vector plotted using meridional wind (v) and vertical velocity (omega) from 1000 hPa to 100 hPa. Values were averaged over longitude 25˚E-45˚E to suit Tanzania. Color contouring represents omega 10^3 ms^{-1}.

the Indian Ocean is said to modify the meridional overturing during ENSO and IOD phases hence affect the global rainfall distribution, including Indian monsoon summer rainfall (Wu & Kirtman, 2004).

4. Conclusion

The study conducted an analysis of the OND IOD-rainfall relationship, focusing on rainfall trends, rainfall patterns, SST patterns, and atmospheric circulations for two distinct time periods: 1976-2010 and 2011-2022. Results from the Sequential Mann-Kendall trend test revealed a notable change in 1976 and 2011. It was also noticed an increase in the correlation between OND IOD and OND rainfall from +0.73 during 1976-2010 to +0.81 during 2011-2022, indicating a strengthening relationship over the study domain.

During positive IOD events, regions that historically received less rainfall experienced significant increase, while areas that typically received abundant rainfall

observed decrease during 2011-2022. Conversely, during negative IOD events, regions that were previously below normal in rainfall experienced above-normal rainfall amounts. These findings suggest a shifting dynamic in the interaction between OND IOD and OND rainfall across the study domain.

Analysis of SST and large-scale atmospheric circulations indicated changes in the relationship between OND IOD and OND rainfall, with a wider warm pool spread over the western Indian Ocean during positive IOD events and stronger cooling over the central Indian Ocean during negative IOD events in the recent period compared to the past. Additionally, shifts in Walker and Hadley circulations further emphasized the altered relationship between OND rainfall and OND IOD.

Overall, the study underscores the strengthened relationship between OND IOD and OND rainfall over Tanzania during 2011-2022 compared to 1976-2010, with implications for seasonal rainfall forecasting and socio-economic impacts. Future research should not only explore the combined influence of ENSO and IOD on OND rainfall but also perform numerical simulation experiments to confirm the observed and proposed physical mechanisms which could then enhance understanding and forecasting capabilities.

In summary, our findings highlight the evolving dynamics of the OND IOD-rainfall relationship, emphasizing the importance of continued monitoring for improved seasonal forecasting and adaptation strategies in Tanzania.

Conflicts of Interest

The authors declare no conflicts of interest regarding the publication of this paper.

References

Ame, H. K., Kijazi, A. L., Changa, L. B., Mafuru, K. B., Ngwali, M. K., Faki, M. M., Hmad, A. O., & Miraji, M. K. (2021). Rainfall Variability over Tanzania during October to December and Its Association with Sea Surface Temperature (SST). *Atmospheric and Climate Sciences, 11,* 324-341. https://doi.org/10.4236/acs.2021.112019

Anande, D. M., & Luhunga, P. M. (2019). Assessment of Socio-Economic Impacts of the December 2011 Flood Event in Dar es Salaam, Tanzania. *Atmospheric and Climate Sciences, 9,* 421-437. https://doi.org/10.4236/acs.2019.93029

Ashok, K., Guan, Z., Saji, N. H., & Yamagata, T. (2004). Individual and Combined Influences of ENSO and the Indian Ocean Dipole on the Indian Summer Monsoon. *Journal of Climate, 17,* 3141-3155. https://doi.org/10.1175/1520-0442(2004)017<3141:IACIOE>2.0.CO;2

Ayugi, B. O., Tan, G., Ongoma, V., & Mafuru, K. B. (2018). Circulations Associated with Variations in Boreal Spring Rainfall over Kenya. *Earth Systems and Environment, 2,* 421-434. https://doi.org/10.1007/s41748-018-0074-6

Black, E., Slingo, J., & Sperber, K. R. (2003). An Observational Study of the Relationship between Excessively Strong Short Rains in Coastal East Africa and Indian Ocean SST. *Monthly Weather Review, 131,* 74-94. https://doi.org/10.1175/1520-0493(2003)131<0074:AOSOTR>2.0.CO;2

Borhara, K., Pokharel, B., Bean, B., Deng, L., & Wang, S.-Y. S. (2020). On Tanzania's Precipitation Climatology, Variability, and Future Projection. *Climate, 8,* Article 34. https://doi.org/10.3390/cli8020034

Chang'a, L. B., Kijazi, A. L., Mafuru, K. B., Kondowe, A. L., Osima, S. E., Mtongori, H. I., Ng'ongolo, H. K., Juma, O. H., & Michael, E. (2020). Assessment of the Evolution and Socio-Economic Impacts of Extreme Rainfall Events in October 2019 over the East Africa. *Atmospheric and Climate Sciences, 10,* 319-338. https://doi.org/10.4236/acs.2020.103018

Clark, C. O., Webster, P. J., & Cole, J. E. (2003). Interdecadal Variability of the Relationship between the Indian Ocean Zonal Mode and East African Coastal Rainfall Anomalies. *Journal of Climate, 16,* 548-554. https://doi.org/10.1175/1520-0442(2003)016<0548:IVOTRB>2.0.CO;2

Harris, I., Osborn, T. J., Jones, P., & Lister, D. (2020). Version 4 of the CRU TS Monthly High-Resolution Gridded Multivariate Climate Dataset. *Scientific Data, 7,* Article No. 109. https://doi.org/10.1038/s41597-020-0453-3

Huang, B., Thorne, P. W., Banzon, V. F., Boyer, T., Chepurin, G., Lawrimore, J. H., Menne, M. J., Smith, T. M., Vose, R. S., & Zhang, H.-M. (2017). Extended Reconstructed Sea Surface Temperature, Version 5 (ERSSTv5): Upgrades, Validations, and Intercomparisons. *Journal of Climate, 30,* 8179-8205. https://doi.org/10.1175/JCLI-D-16-0836.1

Japheth, L. P., Tan, G., Chang'a, L. B., Kijazi, A. L., Mafuru, K. B., & Yonah, I. (2021). Assessing the Variability of Heavy Rainfall during October to December Rainfall Season in Tanzania. *Atmospheric and Climate Sciences, 11,* 267-283. https://doi.org/10.4236/acs.2021.112016

Kalnay, E., Kanamitsu, M., Kistler, R., Collins, W., Deaven, D., Gandin, L., Iredell, M., Saha, S., White, G., Woollen, J., Zhu, Y., Leetmaa, A., Reynolds, R., Chelliah, M., Ebisuzaki, W., Higgins, W., Janowiak, J., Mo, K. C., Ropelewski, C. et al. (1996). The NCEP/NCAR 40-Year Reanalysis Project. *Bulletin of the American Meteorological Society, 77,* 437-471. https://doi.org/10.1175/1520-0477(1996)077<0437:TNYRP>2.0.CO;2

Kavishe, G. M., & Limbu, P. T. S. (2020). Variation of October to December Rainfall in Tanzania and Its Association with Sea Surface Temperature. *Arabian Journal of Geosciences, 13,* Article No. 534. https://doi.org/10.1007/s12517-020-05535-z

Kebacho, L. L. (2021). Anomalous Circulation Patterns Associated with 2011 Heavy Rainfall over Northern Tanzania. *Natural Hazards*, *109,* 2295-2312. https://doi.org/10.1007/s11069-021-04920-5

Kimambo, O. N., Chikoore, H., & Gumbo, J. R. (2019). Understanding the Effects of Changing Weather: A Case of Flash Flood in Morogoro on January 11, 2018. *Advances in Meteorology, 2019,* Article ID: 8505903. https://doi.org/10.1155/2019/8505903

Kistler, R., Collins, W., Saha, S., White, G., Woollen, J., Kalnay, E., Chelliah, M., Ebisuzaki, W., Kanamitsu, M., Kousky, V., van den Dool, H., Jenne, R., & Fiorino, M. (2001). The NCEP-NCAR 50-Year Reanalysis: Monthly Means CD-ROM and Documentation. *Bulletin of the American Meteorological Society, 82,* 247-267. https://doi.org/10.1175/1520-0477(2001)082<0247:TNNYRM>2.3.CO;2

Koutsouris, A. J., Chen, D., & Lyon, S. W. (2016). Comparing Global Precipitation Data Sets in Eastern Africa: A Case Study of Kilombero Valley, Tanzania. *International Journal of Climatology, 36,* 2000-2014. https://doi.org/10.1002/joc.4476

Limbu, P. T. S., & Guirong, T. (2020). Influence of the Tropical Atlantic Ocean and its Walker Circulation Cell on October-December Rainfall Variability over Tanzania. *In-*

ternational Journal of Climatology, 40, 5767-5782. https://doi.org/10.1002/joc.6550

Limbu, P. T. S., & Tan, G. (2019). Relationship between the October-December Rainfall in Tanzania and the Walker Circulation Cell over the Indian Ocean. *Meteorologische Zeitschrift, 28,* 453-469. https://doi.org/10.1127/metz/2019/0939

Lukali, A. A., Osima, S. E., Lou, Y., & Kai, K. H. (2021). Assessing the Impacts of Climate Change and Variability on Maize (*Zea mays*) Yield over Tanzania. *Atmospheric and Climate Sciences, 11,* 569-588. https://doi.org/10.4236/acs.2021.113035

Mafuru, K. B., & Guirong, T. (2020). The influence of ENSO on the Upper Warm Temperature Anomaly Formation Associated with the March-May Heavy Rainfall Events in Tanzania. *International Journal of Climatology, 40,* 2745-2763. https://doi.org/10.1002/joc.6364

Makula, E. K., & Zhou, B. (2022a). Linkage of Tanzania Short Rain Variability to Sea Surface Temperature over the Southern Oceans. *Frontiers in Earth Science, 10,* Article 922172. https://doi.org/10.3389/feart.2022.922172

Mbigi, D., & Xiao, Z. (2021). Analysis of Rainfall Variability for the October to December over Tanzania on Different Timescales during 1951-2015. *International Journal of Climatology, 41,* 6183-6204. https://doi.org/10.1002/joc.7173

Mbigi, D., & Xiao, Z. (2023). Southern Annular Mode: A New Factor Impacts the East African Short Rains after the Early 1990s. *Journal of Climate, 36,* 5511-5525. https://doi.org/10.1175/JCLI-D-22-0613.1

Mosmann, V., Castro, A., Fraile, R., Dessens, J., & Sánchez, J. L. (2004). Detection of Statistically Significant Trends in the Summer Precipitation of Mainland Spain. *Atmospheric Research, 70,* 43-53. https://doi.org/10.1016/j.atmosres.2003.11.002

Otte, I., Detsch, F., Mwangomo, E., Hemp, A., Appelhans, T., & Nauss, T. (2017). Multidecadal Trends and Interannual Variability of Rainfall as Observed from Five Lowland Stations at Mt. Kilimanjaro, Tanzania. *Journal of Hydrometeorology, 18,* 349-361. https://doi.org/10.1175/JHM-D-16-0062.1

Peng, X., Steinschneider, S., & Albertson, J. (2020). Investigating Long-Range Seasonal Predictability of East African Short Rains: Influence of the Mascarene High on the Indian Ocean Walker Cell. *Journal of Applied Meteorology and Climatology, 59,* 1077-1090. https://doi.org/10.1175/JAMC-D-19-0109.1

Prabhu, A., Kripalani, R. H., Preethi, B., & Pandithurai, G. (2016). Potential Role of the February-March Southern Annular Mode on the Indian Summer Monsoon Rainfall: A New Perspective. *Climate Dynamics, 47,* 1161-1179. https://doi.org/10.1007/s00382-015-2894-5

Saji, N. H., Goswami, B. N., Vinayachandran, P. N., & Yamagata, T. (1999). A Dipole Mode in the Tropical Indian Ocean. *Nature, 401,* 360-363. https://doi.org/10.1038/43854

Saji, N., & Yamagata, T. (2003). Possible Impacts of Indian Ocean Dipole Mode Events on Global Climate. *Climate Research, 25,* 151-169. https://doi.org/10.3354/cr025151

Sharma, T., Ratna, S. B., & Pai, D. S. (2023). Modulation of Indian Summer Monsoon Rainfall Response to ENSO in the Recent Decades and Its Large-Scale Dynamics. *Research Square, 1.* https://doi.org/10.21203/rs.3.rs-2405719/v1

Sneyers, R. (1990). *On the Statistical Analysis of Series of Observations.* Technical Note No. 143, World Meteorological Organization.

Thompson, D. W. J., & Wallace, J. M. (2000). Annular Modes in the Extratropical Circulation. Part I: Month-to-Month Variability. *Journal of Climate, 13,* 1000-1016. https://doi.org/10.1175/1520-0442(2000)013<1000:AMITEC>2.0.CO;2

Trenberth, K. E., & Hoar, T. J. (1996). The 1990-1995 El Niño-Southern Oscillation Event: Longest on Record. *Geophysical Research Letters, 23,* 57-60. https://doi.org/10.1029/95GL03602

Umutoni, M. A., Japheth, L. P., Lipiki, E. J., Kebacho, L. L., Limbu, P. T. S., & Makula, E. K. (2021). Investigation of the 2016 March to May extreme rainfall over Rwanda. *Natural Hazards*, *108,* 607-618. https://doi.org/10.1007/s11069-021-04697-7

Vigaud, N., Tippett, M. K., & Robertson, A. W. (2018). Probabilistic Skill of Subseasonal Precipitation Forecasts for the East Africa-West Asia Sector during September-May. *Weather and Forecasting, 33,* 1513-1532. https://doi.org/10.1175/WAF-D-18-0074.1

Wenhaji Ndomeni, C., Cattani, E., Merino, A., & Levizzani, V. (2018). An Observational Study of the Variability of East African Rainfall with Respect to Sea Surface Temperature and Soil Moisture. *Quarterly Journal of the Royal Meteorological Society, 144,* 384-404. https://doi.org/10.1002/qj.3255

Wu, R., & Kirtman, B. P. (2004). Impacts of the Indian Ocean on the Indian Summer Monsoon—ENSO Relationship. *Journal of Climate, 17,* 3037-3054. https://doi.org/10.1175/1520-0442(2004)017<3037:IOTIOO>2.0.CO;2

Xing, L., & Ogou, K. (2015). Influence of Mascarene High and Indian Ocean Dipole on East African Extreme Weather Events. *Geographica Pannonica, 19,* 64-72. https://doi.org/10.5937/GeoPan1502064O

Yamagata, T., Behera, S. K., Luo, J.-J., Masson, S., Jury, M. R., & Rao, S. A. (2013). Coupled Ocean-Atmosphere Variability in the Tropical Indian Ocean. In C. Wang, S. P. Xie, & J. A. Carton (Eds.), *Earth's Climate: The Ocean-Atmosphere Interaction, Volume 147* (pp. 189-211). American Geophysical Union. https://doi.org/10.1029/147GM12